Molecular Genetics and Metabolism 123 (2018) 518–525

Contents lists available at ScienceDirect

Molecular Genetics and Metabolism

journal homepage: www.elsevier.com/locate/ymgme

Regular Article

Developmental dosing with a MEK inhibitor (PD0325901) rescues myopathic features of the muscle-specific but not limb-specific *Nf1* knockout mouse

Matthew A. Summers[a,b], Emily R. Vasiljevski[a,b], Kathy Mikulec[a], Lauren Peacock[a], David G. Little[a,b], Aaron Schindeler[a,b,*]

[a] Orthopaedic Research & Biotechnology, The Children's Hospital at Westmead, Westmead, NSW, Australia
[b] Discipline of Paediatrics & Child Heath, Faculty of Medicine, University of Sydney, Camperdown, NSW, Australia

ARTICLE INFO

Keywords:
Neurofibromatosis type 1 (NF1)
Muscle weakness
Myopathy
MEK inhibitor

ABSTRACT

Neurofibromatosis Type 1 (NF1) is a common autosomal dominant genetic disorder While NF1 is primarily associated with predisposition for tumor formation, muscle weakness has emerged as having a significant impact on quality of life. NF1 inactivation is linked with a canonical upregulation Ras-MEK-ERK signaling. This in this study we tested the capacity of the small molecule MEK inhibitor PD0325901 to influence the intramyocellular lipid accumulation associated with NF1 deficiency. Established murine models of tissue specific *Nf1* deletion in skeletal muscle ($Nf1_{MyoD}^{-/-}$) and limb mesenchyme ($Nf1_{Prx1}^{-/-}$) were tested.

Developmental PD0325901 dosing of dams pregnant with $Nf1_{MyoD}^{-/-}$ progeny rescued the phenotype of day 3 pups including body weight and lipid accumulation by Oil Red O staining. In contrast, PD0325901 treatment of 4 week old $Nf1_{Prx1}^{-/-}$ mice for 8 weeks had no impact on body weight, muscle wet weight, activity, or intramyocellular lipid. Examination of day 3 $Nf1_{Prx1}^{-/-}$ pups showed differences between the two tissue-specific knockout strains, with lipid staining greatest in $Nf1_{MyoD}^{-/-}$ mice, and fibrosis higher in $Nf1_{Prx1}^{-/-}$ mice.

These data show that a MEK/ERK dependent mechanism underlies NF1 muscle metabolism during development. However, crosstalk from *Nf1*-deficient non-muscle mesenchymal cells may impact upon muscle metabolism and fibrosis in neonatal and mature myofibers.

1. Introduction

Neurofibromatosis Type 1 (NF1) is an autosomal dominant genetic disease associated with multi-system manifestations, including a predisposition to tumor formation [1,2], cognitive developmental delays affecting executive functions [3,4], and a range of musculoskeletal abnormalities [5,6]. Early reports of motor deficits in NF1 children were attributed to dysfunction in the central nervous system [7]. However, recent clinical studies have identified features suggestive of a primary myopathy having substantial impact on individual quality of life [6]. Reports of reduced muscle size [8], impaired exercise capacity [9,10], and muscle weakness [9,11–13] align with anecdotal reports from parents and clinicians describing fatigability and weakness as relevant disease features. Notably, a 2015 study reports 30–50% reduced muscle strength in isolated upper and lower limb muscles of NF1 children when compared to matched controls [11]. Collectively these data shifted the paradigm towards NF1 having a primary role in muscle development, function, and/or maintenance.

Initial genetic studies defined the *NF1* protein product neurofibromin as a RasGTPase-activating protein (GAP) and a regulator of the classic Ras-MAPK (mitogen-activated-protein-kinase) signaling cascades [14,15]. Notably, biochemical and genetic studies suggest a critical role for NF1-MAPK signaling in the regulation in muscle development [16–18]. For example, neurofibromin was found to be up regulated during myoblast differentiation [18], and accordingly, increased MAPK signaling in engineered myoblasts expressing GAP-resistant H-Ras showed impaired myotube differentiation [19]. In mice, global *Nf1* inactivation is embryonic lethal and mutant embryos show impaired cardiac and skeletal muscle development [16].

More recent work using conditional knockout mice indicate a critical role for the NF1-MAPK pathway in muscle energy metabolism. For example, muscle-specific inactivation of murine *Nf1* using the *MyoD-Cre* transgene ($Nf1_{MyoD}^{-/-}$) resulted in substantial intramyocellular lipid accumulations in neonatal muscle [20]. Parallel analyses of tissue from the limb-specific *Nf1* knockout mouse ($Nf1_{Prx1}^{-/-}$) found similarly elevated muscle lipid levels, along with alterations in

* Corresponding author at: Orthopaedic Research & Biotechnology, Research Building, The Children's Hospital at Westmead, Locked Bag 4001, Westmead, NSW 2145, Australia.
E-mail address: aaron.schindeler@sydney.edu.au (A. Schindeler).

https://doi.org/10.1016/j.ymgme.2018.02.009
Received 12 January 2018; Received in revised form 15 February 2018; Accepted 15 February 2018
Available online 16 February 2018

mitochondrial metabolic enzyme activity [20]. Intramyocellular lipid accumulation is a pathological feature of a group of genetic disorders known as lipid storage myopathies [21]. These include Primary Carnitine Deficiency (PCD), Multiple Acyl-CoA Dehydrogenase Deficiency (MADD) and Neutral Lipid Storage Disease (NLSD). All of these disorders have been associated with mutations in enzymes specifically involved in triglyceride metabolism, resulting in the build-up of lipid within muscle fibers and clinically manifesting as muscle weakness, myalgia or extreme fatigue.

The function and relative significance of NF1-Ras-MAPK signaling is largely unknown in the context muscle, however studies outside of NF1 provide key insight. For example, molecular studies of the active MEK kinase (a MAPK intermediate) show its inhibitory effects on the myogenic regulatory factor *MyoD*, and suggest control of MEK phosphorylation is critical for the transactivation of myogenic genes [22]. Clinical data further corroborate these findings. When small molecule MEK inhibitors (MEKi) PD98059 and Selumetinib (AZD6244) have been used to treat malignant tumors, secondary increases in skeletal muscle mass were observed in both mice [23] and humans [24].

PD0325901 represents one of the most potent and specific inhibitors of MEK-ERK signaling (K_i of 1 nM against activated MEK1 and MEK2 in vitro) and functions as a non-ATP competitive inhibitor [25]. In preclinical murine models of NF1, the PD0325901 was found to enhance bone formation in a tibial pseudarthrosis setting [26] and to suppress growth of malignant-peripheral nerve sheath tumors (MPNST) [27]. PD0325901 is currently in phase-2 clinical trial for the treatment of plexiform neurofibromas https://clinicaltrials.gov/ct2/show/NCT02096471. However, the ability of MEK inhibitors to ameliorate muscle development and/or function in NF1 is yet to be trialed.

In this study, we first aimed to assess the ability of (PD0325901) treatment to rescue the severe myopathic phenotype of $Nf1_{MyoD}^{-/-}$ neonatal mice. Next, we examined parallel myopathic features between neonatal $Nf1_{Prx1}^{-/-}$ and neonatal $Nf1_{MyoD}^{-/-}$ muscle. And lastly, we test the capacity of PD0325901 treatment to reverse an established myopathy using the $Nf1_{Prx1}^{-/-}$ line, which lacks *Nf1* in the limbs. These mouse lines and their phenotypes are reviewed in [6].

2. Results

2.1. Developmental dosing with PD0325901 rescues myopathic features of neonatal $Nf1_{MyoD}^{-/-}$ mice

To test the hypothesis that the development of intramyocellular lipid deposits in $Nf1_{MyoD}^{-/-}$ mice is MAPK/ERK signaling dependent, pregnant females bearing $Nf1_{MyoD}^{-/-}$ pups were orally dosed with 5 mg/kg/day PD0325901 via jelly feeding from ED9.5. This PD0325901 delivery method has been previously validated by us in the context of fracture healing models [26]. Pups were born and culled 3 days after birth, and tissues were harvested for analysis. Primary outcome measures were changes in body weight and muscle lipid accumulation.

Embryonic dosing with PD0325901 resulted in an increase in bodyweight of $Nf1_{MyoD}^{-/-}$mice at day 3 compared with those untreated (Fig. 1A). Notably, while pup bodyweight was not completely restored to WT levels, a significant effect of treatment was still observed between $Nf1_{MyoD}^{-/-}$ groups (Fig. 1A). Subsequent histological analysis of muscle tissues using Oil Red O found a striking 56% reduction in lipid staining in muscle cross sections (mid-belly of the quadriceps) of treated mice (Fig. 1B–C). Representative images illustrated the dramatic reduction in staining to WT levels (Fig. 1C). Subsequent western blot analyses of treated dam tissues confirmed daily dosing with PD0325901 results in substantial knockdown of signaling through the MAPK/MEK/ERK cascade, shown by the substantial reductions in ERK phosphorylation levels (Supplementary Fig. 1). Consistent with our previous report, there was observed changes in myofiber cross-section or sarcomeric structure [20].

2.2. PD0325901 dosing (pre- and post-natal) does not rescue myopathic features of the $Nf1_{Prx1}^{-/-}$ mouse

While the $Nf1_{MyoD}^{-/-}$ mouse model is ideal for developmental studies, the high neonatal lethality prior to day 7 prevents testing therapeutics in adult $Nf1^{null}$ muscle in this mouse line [20]. Thus, to assess the ability of PD0325901 treatment to reverse the muscle phenotype in mature muscle, we adopted the $Nf1_{Prx1}^{-/-}$ mouse. This strain survives post-weaning, and presents with reduced bodyweight, reduced muscle size, and muscle weakness [28].

An assessment of neonatal $Nf1_{Prx1}^{-/-}$ and $Nf1_{MyoD}^{-/-}$ tissues was first performed to compare their respective phenotypic features. $Nf1_{Prx1}^{-/-}$ neonates were bred and culled prior to weaning, and tissues were assessed for features of myopathy at day 3 post-birth. In line with data from the $Nf1_{MyoD}^{-/-}$ strain, $Nf1_{Prx1}^{-/-}$ neonates were significantly smaller at day 3 compared to littermate controls (Fig. 2A). Histological analysis of neonatal muscle using H&E staining found substantial endomysial fibrosis and infiltrating mononuclear cells throughout the muscle belly (Fig. 2B). Representative whole tissue sections show the striking phenotypic differences at both the macroscopic (2×) and microscopic (20×) levels (Fig. 2B). Assessment of muscle lipid accumulation by Oil Red O staining confirmed focal regions of increased lipid in $Nf1_{Prx1}^{-/-}$ neonatal muscle fibers (Fig. 2B).

Next, $Nf1_{Prx1}^{-/-}$ mice from 4 weeks of age were treated with PD0325901 to assess any effects of therapeutic reversal. Mice were dosed orally with 5 mg/kg/day PD0325901 via jelly feeding. Dosing continued for 8 consecutive weeks and mice were culled at 12 weeks of age for analysis. Primary outcome measures included changes in bodyweight, changes in isolated muscle weight, muscle histopathology, and functional muscle measures of grip strength and activity via open field testing.

Measures of bodyweight, grip strength, and muscle weight, were all significantly higher for WT mice compared with either untreated or treated $Nf1_{Prx1}^{-/-}$ mice (Fig. 3A–C). No effect of PD0325901 treatment between $Nf1_{Prx1}^{-/-}$ groups could be detected by analysis-of-variance (ANOVA) with multiple comparisons (Fig. 3A–C). Similarly, functional assessment of physical activity and fatigue using open-field testing found no detectable effects of PD0325901 treatment on the number of hind-limb rears (Fig. 3D), total distance travelled (Fig. 3E), or total activity (Fig. 3F) within a 15 min period. A subsequent histological analysis of muscle tissues using H&E and Oil Red O confirmed that the myopathic features of endomysial fibrosis and focal lipid accumulations seen in neonates remained present in adult muscle, and were not appreciably effected by PD0325901 treatment (Fig. 3G).

To determine whether the differences between neonatal $Nf1_{MyoD}^{-/-}$ and mature $Nf1_{Prx1}^{-/-}$ mice were attributable to strain or timing differences, a group of $Nf1_{Prx1}^{-/-}$ pups were culled 3 days after birth, with dams having been treated during pregnancy with PD0325901 or vehicle. $Nf1_{Prx1}^{-/-}$ neonates show decreased body weight compared to wild type pups, however despite very limited numbers of live $Nf1_{Prx1}^{-/-}$ neonates from dams receiving PD0325901 treatment, the body weight of surviving pups was not improved (Fig. 4A). Critically, unlike the $Nf1_{MyoD}^{-/-}$ neonates and similar to the $Nf1_{Prx1}^{-/-}$ adults, no qualitative changes in intramyocellular lipid was seen by Oil Red O staining with PD0325901 treatment (Fig. 4B).While intramyocellular lipid was less in neonatal $Nf1_{Prx1}^{-/-}$ muscle compared to that previously described in $Nf1_{MyoD}^{-/-}$ specimens, both control and PD0325901 treated samples showed high fibrosis (Fig. 4B).

3. Discussion

In this study we have shown that PD0325901, a pathway specific MEK inhibitor, can modify the developmental muscle phenotype of the $Nf1_{MyoD}^{-/-}$ mouse, but not the $Nf1_{Prx1}^{-/-}$ mouse. These findings highlight the critical role of Ras-MEK/ERK signaling in muscle development, but also potentially indicate crosstalk from $Nf1^{null}$ non-muscle

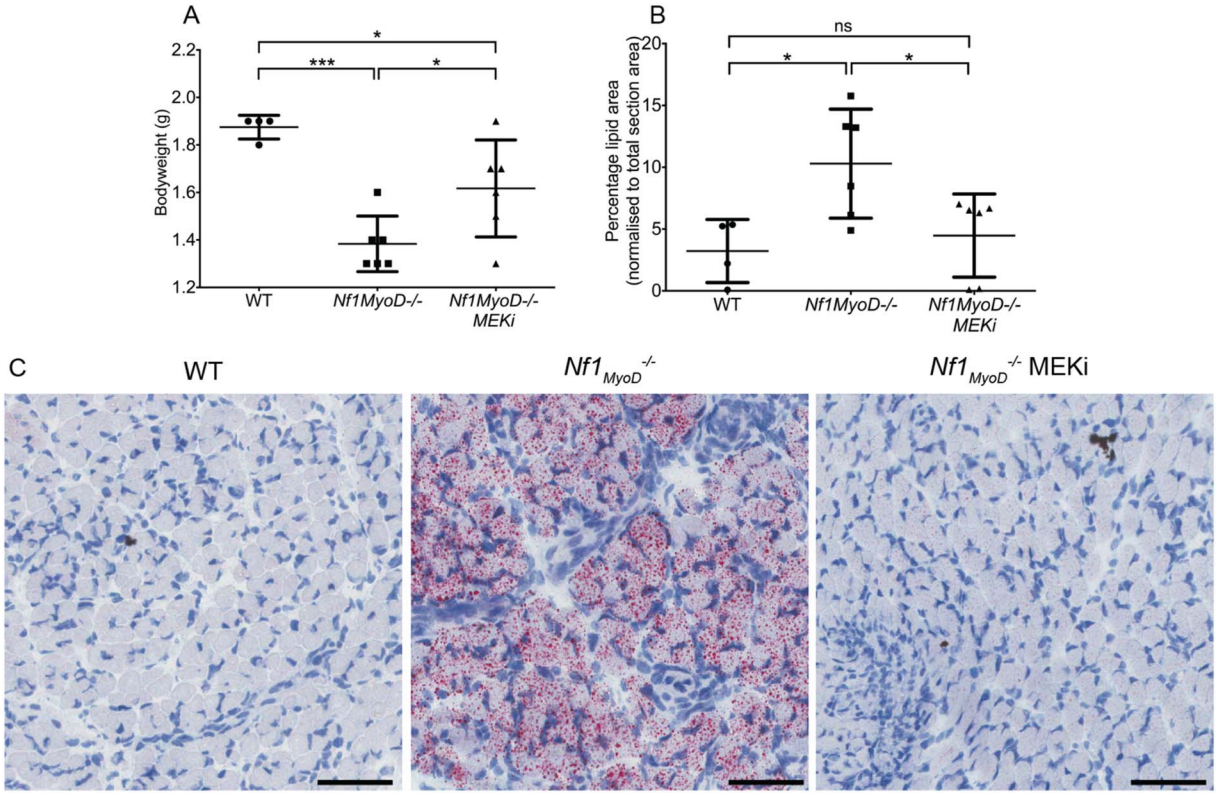

Fig. 1. Developmental dosing with PD0325901 (MEKi) from ED9.5 rescued the myopathic features of the $Nf1_{MyoD}{}^{-/-}$ mouse. (A) Bodyweight of 3 day old pups following developmental dosing with 5 mg/kg/day PD0325901 shows a significant increase in $Nf1_{MyoD}{}^{-/-}$ mice compared to vehicle treated controls. (B–C) Histological analysis using Oil Red O revealed a mean 56% reduction in intramyocellular lipid staining in mid-belly muscle cross sections (n = 6) compared with vehicle treated animals (n = 6). Scale bars: 200 μm. Data are presented as mean ± SD. Statistical testing was done using ANOVA with Dunn's multiple comparisons testing. *$P < .05$, ***$P < .001$, ns (not significant, $P > .05$). (For interpretation of the references to colour in this figure legend, the reader is referred to the web version of this article.)

tissues in the $Nf1_{Prx1}{}^{-/-}$ can influence the murine phenotype. Such a phenomenon has been previously reported to affect the NF1 tumor microenvironment, with signaling from $Nf1^{+/-}$ fibroblasts affecting $Nf1^{-/-}$ neurofibroma cells [29].

Several lines of evidence suggest that the initiation and progression of the myogenic program is critically regulated by the Ras-MAPK/ERK cascade. Notably, in vitro myoblast experiments have demonstrated that impaired myoblast differentiation following Ras activation is independent of Pi3K-AKT signaling [19,30], and is instead mediated via the MEK/ERK dependent modulation of key factors such as *MyoD* [22] and the myosin heavy-chain promotors [30]. In mice, increased myofiber ERK phosphorylation and impaired myoblast differentiation was seen in embryonic muscle following *Nf1* inactivation [28], however, in adult muscle from the same strain, ERK activation was normal [28]. Collectively these data align with descriptions of the inhibition of MAPK/ERK signaling by Pi3K-AKT late in the myogenic program [30], and could explain the redundancy of PD0325901 treatment in post mitotic $Nf1^{null}$ muscle.

Genetic and/or developmental differences between the $Nf1_{MyoD}{}^{-/-}$ and $Nf1_{Prx1}{}^{-/-}$ strains also needs to be considered. *Prx1*-cre expression is most active in the hind limbs from ED10.5–11 [31], approximately 1.5 developmental days after *MyoD*-cre [32]. Thus, by this developmental time Ras-MAPK/ERK signaling may be differentially required. Indeed, we have previously noted substantial differences in outcomes between strains [20]. For example, elevated activity of mitochondrial enzymes citrate synthase (CS), succinate dehydrogenase (SDH), beta-hydroxyacyl-CoA dehydrogenase (BHAD), and medium-chain Acyl-CoA dehydrogenases (MCAD) was present in $Nf1_{Prx1}{}^{-/-}$ muscle, but not in extracts from $Nf1_{MyoD}{}^{-/-}$ mice [20]. We have speculated that this enzyme upregulation in $Nf1_{Prx1}{}^{-/-}$ mice may be compensatory [20], and may assist with the compensatory clearing of intramyocellular lipid.

Differences between affected muscle groups as well as the efficiency of Cre-mediated recombination may also be contributing. *MyoD*-Cre drives inactivation in all skeletal muscle precursors, and thus all developing body and limb skeletal muscles. In contrast, *Prx1*-Cre expression targets the fore and hind limbs [31], leaving the axial musculature genetically normal and this could provide a level of metabolic compensation. The *Prx1*-Cre transgene may also be less efficient, as PCR of a range of muscle groups in the $Nf1_{Prx1}{}^{-/-}$ mice shows a residual presence of the non-excised allele [28]. Together, these may explain the increased survivability of $Nf1_{Prx1}{}^{-/-}$ mice [20], as well as differences in lipid accumulation and mitochondrial enzyme activity.

The capacity of MEKi to improve fracture healing in NF1 models of pseudarthroses is relevant to consider in the context of this study [33]. Fracture healing recapitulates many of the cellular processes that occur during skeletal development [34]. This further reflects the critical role for *NF1* in developmental rather than post-mitotic cell biology. For example, adult $Nf1^{+/-}$ mice have significantly impaired rates of bone healing following fracture [35], however, in the absence of fracture $Nf1^{+/-}$ bones appear normal [20]. Similarly, the reported increases in muscle mass following MEKi dosing in cancer patients [24] likely reflects the mitigation of muscle wasting through an increased rate of muscle repair; a process recapitulating embryonic myogenesis involving the progressive fusion of muscle stem cells [32,36]. While MEKi treatment improved bone healing outcomes in $Nf1^{null}$ fractures, its notable that treatment had no effect on fibrotic tissue infiltrate in the above-mentioned study [33].

A well-described limitation of the $Nf1_{Prx1}{}^{-/-}$ model is that they have reduced size, body weight, and can develop fused joints during development [28]. This can have a significant impact on animal activity, and may in combination with reduced muscle mass contribute to

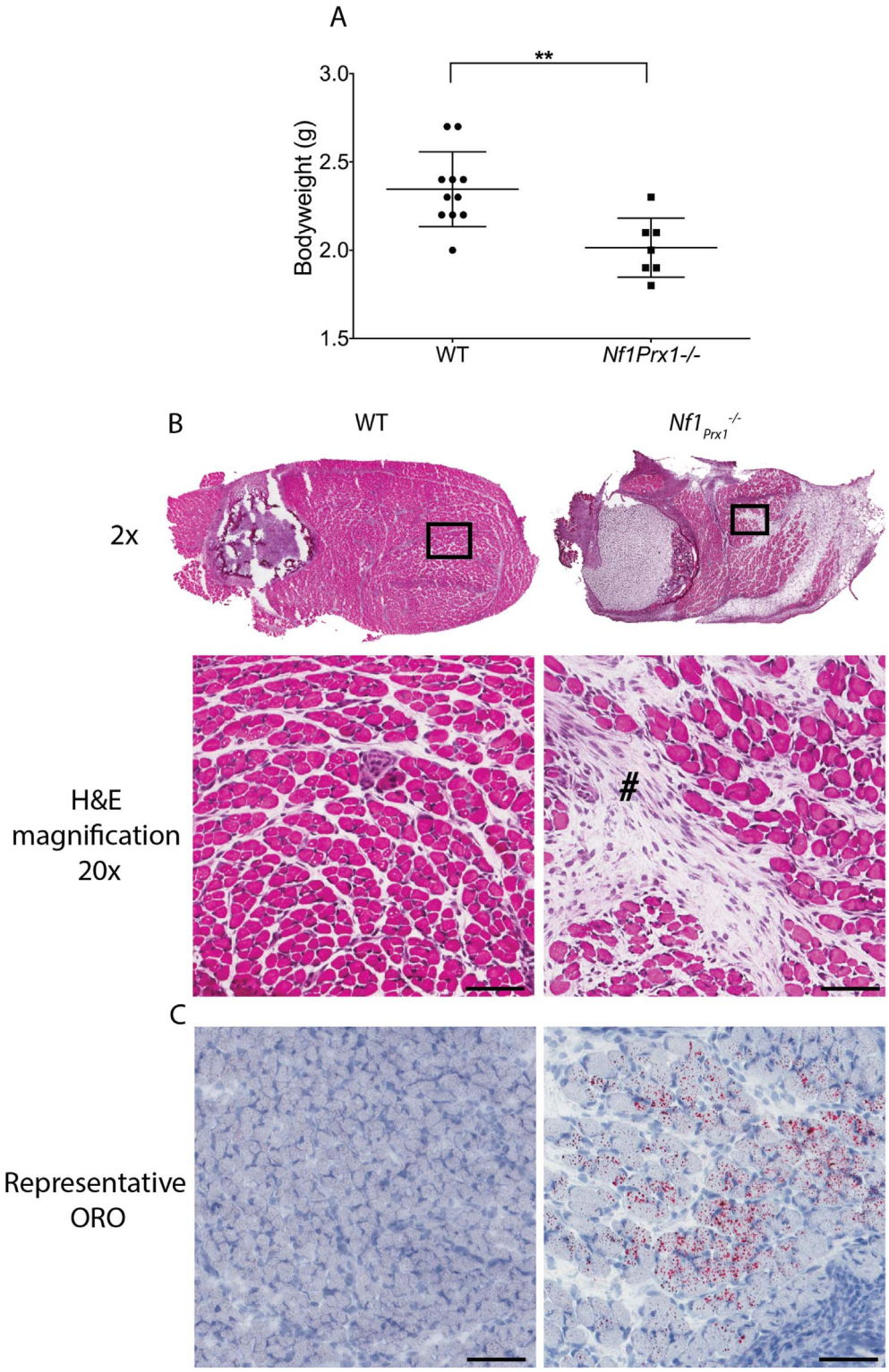

Fig. 2. $Nf1_{Prx1}{}^{-/-}$ mice show a neonatal myopathy. (A) The bodyweight of the $Nf1_{Prx1}{}^{-/-}$ mice were significantly reduced at day 3 compared to littermate controls. (B) Representative images 8 week limb muscle with H&E staining highlighting fibrosis and mononuclear cell infiltration (#) at the macroscopic (2×) and microscopic (20×) levels. (C) Neutral lipid staining by Oil Red illustrates lipid deposited in neonatal muscle fibers. Scale bars; 200 μm. Data are presented as mean ± SD. Statistical testing was done using parametric Students *t*-test. $^{**}P < .01$. (For interpretation of the references to colour in this figure legend, the reader is referred to the web version of this article.)

measures such as grip strength. However, in a recent study, this model was effectively used to test an enriched medium chain fatty acid and carnitine supplemented diet; significant changes in grip strength and intramyocellular lipid were seen with this treatment in the $Nf1_{Prx1}{}^{-/-}$ mouse [37].

Increased muscle fibrosis has been previously reported in $Nf1_{Prx1}{}^{-/-}$ mice [28], and remained unaffected by PD0325901 treatment in our study (Fig. 3) and was described for the first time in early neonatal muscle (Fig. 4B). This suggests a MEK/ERK independent regulatory mechanism in this mesenchymal cell subtype. Indeed, negligible muscle fibrosis is observed in the muscle-specific $Nf1_{MyoD}{}^{-/-}$ knockout mouse [20], suggesting tissue-specific roles for *NF1* and Ras/MAPK signaling

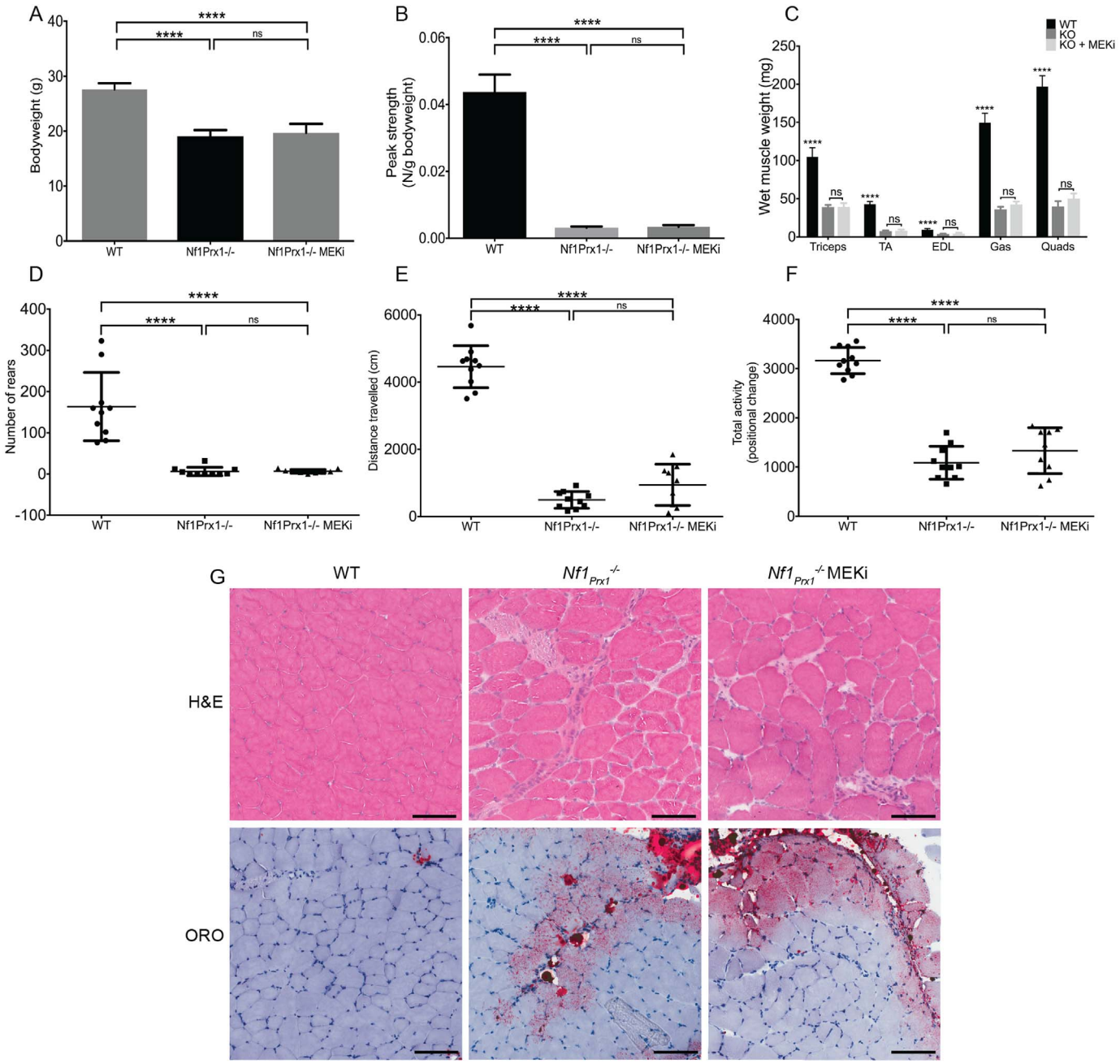

Fig. 3. PD0325901 (MEKi) dosing does not modify the muscle phenotype of adult $Nf1_{Prx1}{}^{-/-}$ mice. (A) Bodyweight, (B) grip strength, and (C) muscle weights of WT mice were all significantly higher than $Nf1_{Prx1}{}^{-/-}$ mice across both groups. (D–E) Open field testing measures of (D) the number of hind limb rears, (E) total distance travelled, and (F) total activity found no effect of PD0325901 treatment. n = 10 for all measures. (G) Representative histological images showed no significant effects of treatment on endomysial fibrosis or focal neutral lipid staining. Scale bars: 200 μm. Data are presented as mean ± SD. Statistical testing was done using ANOVA with Dunn's multiple comparisons testing. ****$P < .0001$, ns (not significant).

in non-muscle mesenchymal cells, such as fibroblasts. This may be attributable to tissue-specific isoforms of *NF1* [17,38], whose differential function remains unclear.

Current clinical evidence indicates that NF1-associated muscle dysfunction does not feature by muscle wasting, but is rather characterized by a combination of metabolic weakness and fatigability [6]. Indeed, $Nf1_{MyoD}{}^{-/-}$ knockout muscle has been recently demonstrated to have impaired long-chain fatty acid metabolism, which could be rescued in $Nf1_{Prx1}{}^{-/-}$ mice by a diet lower in long-chain fatty acids [37]. In conclusion, exploring the mechanism underlying the NF1-Ras-MAPK dependency of altered fatty acid metabolism represents a key area for future NF1 muscle research.

4. Materials and methods

4.1. Mouse strains and husbandry

Animal experiments were approved by the Westmead Hospital Animal Ethics Committee or the Children's Hospital at Westmead/Children's Medical Research Institute Animal Ethics Committee. The *MyoD-Cre* transgenic mice were a gift from Prof David Goldhamer (University of Connecticut, CN, USA). $Nf1_{MyoD}{}^{-/-}$ mice [20] were generated by an F1 cross of *MyoD-Cre* and $Nf1^{flox}$ mice to produce $MyoD\text{-}Cre^{+/-}$ $Nf1^{flox/+}$ mice. They were then backcrossed to the parental $Nf1^{flox/flox}$ strain to generate experimental homozygous (F2) knockout animals $MyoD\text{-}Cre^{+/-}$ $Nf1^{flox/flox}$ ($Nf1_{MyoD}{}^{-/-}$).

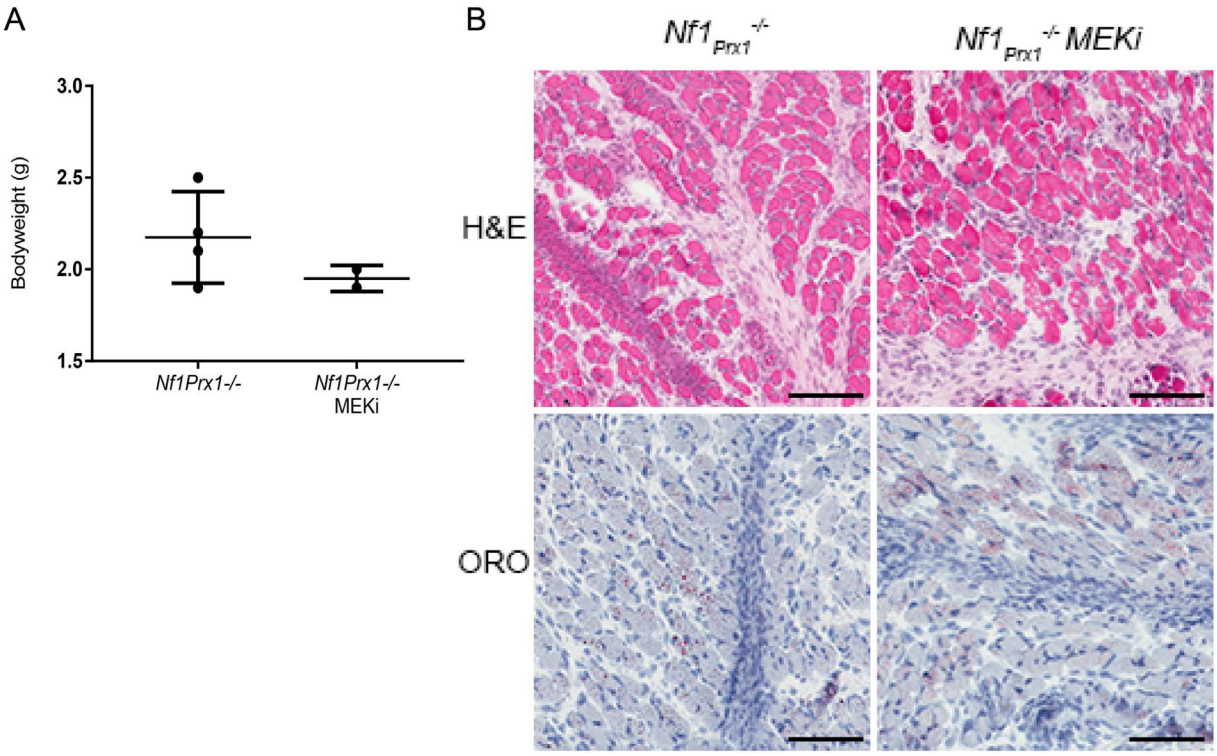

Fig. 4. Developmental dosing with PD0325901 (MEKi) from ED9.5 did not rescue the myopathic features of the $Nf1_{Prx1}{}^{-/-}$ mouse (A) Bodyweight of 3 day old pups following developmental dosing with 5 mg/kg/day PD0325901 does not show an increase in $Nf1_{Prx1}{}^{-/-}$ mice compared to vehicle treated controls. (B) Histological analysis revealed no reduction in fibrosis and cell infiltration by H&E, and intramyocellular lipid by Oil Red O in mid-belly muscle cross sections of treated animals (n = 2) compared with vehicle treated animals (n = 4). Scale bars: 200 μm. Data are presented as mean ± SD. Statistical testing was done using an unpaired *t*-test (not significant $P > .05$). (For interpretation of the references to colour in this figure legend, the reader is referred to the web version of this article.)

Prx1-Cre transgenic mice [31] and $Nf1^{flox/flox}$ mice [39] (sourced from the NIH) were crossed to produce first generation *Prx1-Cre*$^{+/-}$ $Nf1^{flox/+}$ mice. They were then backcrossed to the parental $Nf1^{flox/flox}$ strain to generate experimental homozygous knockout animals *Prx1 Cre*$^{+/-}$ $Nf1^{flox/flox}$ ($Nf1_{Prx1}{}^{-/-}$) [28].

$Nf1_{Prx1}{}^{-/-}$ mice were distinctly smaller than their littermates. To ensure their survival and reduce maternal rejection for adult studies, smaller pups were given daily saline injections of 0.05–0.1 mL until bodyweight normalisation. Samples were collected at two weeks of age for genotyping by quantitative real-time PCR for the *Cre* and $Nf1^{flox}$ alleles (Transnet YX, U.S.A). All colonies were maintained on a C57/B6 background.

4.2. PD0325901 dosing

PD0325901 was delivered to the mice orally via feeding of strawberry-flavoured jelly. This jelly was composed of 0.8% DMSO (Sigma-Aldrich) with or without PD0325901 (Selleck Chemicals) dissolved, 16% SPLENDA low Calorie Sweetener (Johnson & Johnson Pacific, New South Wales, Australia), 9.6% gelatin to maintain jelly shape (GELITA Australia, New South Wales, Australia), and 7.9% flavouring (QUEEN Flavouring Essence Imitation Strawberry, Queen Fine Foods, Queensland, Australia). Single housing of the mice assured that the jelly was being consumed. This method has been previously published [26].

4.3. Histological staining

Neonatal hind limbs were harvested from animals at cull, surface coated in Tissue-Tek® O.C.T. Compound (Sakura Finetek USA), placed on a thin piece of tin foil, frozen in isopentane (2-methyl butane) supercooled in liquid nitrogen, and stored at −80 °C. Sections 8 μm thick were cut on a Leica CM1950 Clinical Cryostat, captured on Superfrost™ Plus Microscope Slides (Fisher Scientific, USA), and stored at 4 °C prior to staining.

H&E and Oil Red O staining were performed as previously published [20]. Quantification was performed using Fiji ImageJ [40], by measuring total lipid stained (red) area as a percentage of the total section area.

4.4. Western blotting and antibodies

Western blots were performed on muscle lysates from MEKi treated and untreated mice. Muscle tissues were cryosectioned (15–20 × 8 μm sections) and collected for solubilization. Samples were lysed by agitation at 4 °C for 30 min in RIPA Buffer (Sigma R0278) with protease (Sigma P8340) and phosphatase (Sigma P5726) inhibitors added. Total protein content was determined using a BCA assay kit (Pierce 23,225) with a BSA standard curve. Samples were then heated to 94 °C for 3 min and prepared for loading. Twenty microgram of total protein/sample was run on 4–20% polyacrylamide precast gels (Bio-Rad) in Tris-Glycine buffer. Proteins were transferred to PVDF membrane. Antibodies used for Western blotting were Phospho-p44/42 MAPK (Erk1/2) (Thr202/Tyr204) (Cell Signaling Antibody #9101) 1:2000, and p44/42 MAPK (Erk1/2) (Cell signaling Antibody #9102) 1:2000.

4.5. Grip strength testing

Grip strength testing was performed using a specialty mouse grip strength tester (Columbus instruments). Grip strength (peak force in Newtons) was measured in 3 sets of 5 efforts, with a 20 s rest between sets; for a total of 15 measures. The highest and lowest readings were excluded, and remaining readings were averaged. To ensure unbiased reliable testing, an experienced technician performed all testing for the study duration and was blinded to treatment group and mouse genotype.

4.6. Open field-testing

Open field measurements were performed using an infrared (IR) Actimeter (PanLab Harvard Apparatus). Mice cages were placed in the testing room and left for 30 min to acclimatize to room conditions. At initiation of testing, one mouse is placed in the centre of the open field and allowed to voluntarily explore undisturbed for a 15 min period. Movement data are automatically and electronically recorded by the IR sensors and PanLab software, and exported for analysis. The field cage is thoroughly cleaned using ethanol between each mouse tested.

4.7. Statistical analysis

Biological and technical replicates were conducted at least 3 times for all histological staining experiments. Experimental results are expressed as mean ± standard deviation (unless otherwise specified). Where 2 groups were compared, statistical comparisons were made using parametric two-tailed Student's *t*-tests. Multiple group comparisons were done using ANOVA with a Dunn's *post-hoc* multiple comparisons test. *P*-values of < 0.05 were considered statistically significant.

Acknowledgments

This study was carried out with funding support from the Children's Tumor Foundation (2013B-05-009) and the United States Department of Defense funding (NF130064_nl). Matthew Summers was supported by an Australian Postgraduate Award (APA) and Emily Vasiljevski by an Australian Government Research Training Program (RTP) Scholarship.

Conflicts of interest

Authors have no conflicts of interest to declare.

Appendix A. Supplementary data

Supplementary data to this article can be found online at https://doi.org/10.1016/j.ymgme.2018.02.009.

References

[1] N. Ratner, S.J. Miller, A RASopathy gene commonly mutated in cancer: the neurofibromatosis type 1 tumour suppressor, Nat. Rev. Cancer 15 (2015) 290–301.
[2] R.E. Ferner, D.H. Gutmann, Neurofibromatosis type 1 (NF1): diagnosis and management, Handb. Clin. Neurol. 115 (2013) 939–955.
[3] A. Lehtonen, E. Howie, D. Trump, S.M. Huson, Behaviour in children with neurofibromatosis type 1: cognition, executive function, attention, emotion, and social competence, Dev. Med. Child Neurol. 55 (2013) 111–125.
[4] T.M. Levine, A. Materek, J. Abel, M. O'Donnell, L.E. Cutting, Cognitive profile of neurofibromatosis type 1, Semin. Pediatr. Neurol. 13 (2006) 8–20.
[5] N.B. Patel, G.S. Stacy, Musculoskeletal manifestations of neurofibromatosis type 1, AJR Am. J. Roentgenol. 199 (2012) W99–106.
[6] M.A. Summers, K.G. Quinlan, J.M. Payne, D.G. Little, K.N. North, A. Schindeler, Skeletal muscle and motor deficits in neurofibromatosis type 1, J. Musculoskelet. Neuronal Interact. 15 (2015) 161–170.
[7] R. Feldmann, J. Denecke, M. Grenzebach, G. Schuierer, J. Weglage, Neurofibromatosis type 1: motor and cognitive function and T2-weighted MRI hyperintensities, Neurology 61 (2003) 1725–1728.
[8] D.A. Stevenson, L.J. Moyer-Mileur, J.C. Carey, J.L. Quick, C.J. Hoff, D.H. Viskochil, Case-control study of the muscular compartments and osseous strength in neurofibromatosis type 1 using peripheral quantitative computed tomography, J. Musculoskelet. Neuronal Interact. 5 (2005) 145–149.
[9] B.A. Johnson, B. Macwilliams, J.C. Carey, D.H. Viskochil, J.L. D'Astous, D.A. Stevenson, Lower extremity strength and hopping and jumping ground reaction forces in children with neurofibromatosis type 1, Hum. Mov. Sci. 31 (2012) 247–254.
[10] J.F. de Souza, C.G. Araujo, N.A. de Rezende, L.O. Rodrigues, Exercise capacity impairment in individuals with neurofibromatosis type 1, Am. J. Med. Genet. A 161a (2013) 393–395.
[11] K.M. Cornett, K.N. North, K.J. Rose, J. Burns, Muscle weakness in children with neurofibromatosis type 1, Dev. Med. Child Neurol. 57 (2015) 733–736.
[12] D.A. Stevenson, S. Allen, W.E. Tidyman, J.C. Carey, D.H. Viskochil, A. Stevens, H. Hanson, X. Sheng, B.A. Thompson, M.J. Okumura, K. Reinker, B. Johnson, K.A. Rauen, Peripheral muscle weakness in RASopathies, Muscle Nerve 46 (2012) 394–399.
[13] J.F. Souza, R.L.F. Passos, A.C.M. Guedes, N.A. Rezende, L.O.C. Rodrigues, Muscular force is reduced in neurofibromatosis type 1, J. Musculoskelet. Neuronal Interact. 9 (2009) 15–17.
[14] A. Klose, M.R. Ahmadian, M. Schuelke, K. Scheffzek, S. Hoffmeyer, A. Gewies, F. Schmitz, D. Kaufmann, H. Peters, A. Wittinghofer, P. Nurnberg, Selective disactivation of neurofibromin GAP activity in neurofibromatosis type 1, Hum. Mol. Genet. 7 (1998) 1261–1268.
[15] J.E. DeClue, B.D. Cohen, D.R. Lowy, Identification and characterization of the neurofibromatosis type 1 protein product, Proc. Natl. Acad. Sci. U. S. A. 88 (1991) 9914–9918.
[16] C.I. Brannan, A.S. Perkins, K.S. Vogel, N. Ratner, M.L. Nordlund, S.W. Reid, A.M. Buchberg, N.A. Jenkins, L.F. Parada, N.G. Copeland, Targeted disruption of the neurofibromatosis type-1 gene leads to developmental abnormalities in heart and various neural crest-derived tissues, Genes Dev. 8 (1994) 1019–1029.
[17] D.H. Gutmann, R.T. Geist, K. Rose, D.E. Wright, Expression of two new protein isoforms of the neurofibromatosis type 1 gene product, neurofibromin, in muscle tissues, Dev. Dyn. 202 (1995) 302–311.
[18] D.H. Gutmann, J.L. Cole, F.S. Collins, Modulation of neurofibromatosis type 1 gene expression during in vitro myoblast differentiation, J. Neurosci. Res. 37 (1994) 398–405.
[19] M. Karasarides, K. Dee, D. Schulman, A. Wolfman, C.M. Weyman, Active Ras-induced effects on skeletal myoblast differentiation and apoptosis are independent of constitutive PI3-kinase activity, Cell Biol. Int. 30 (2006) 308–318.
[20] K. Sullivan, J. El-Hoss, K.G. Quinlan, N. Deo, F. Garton, J.T. Seto, M. Gdalevitch, N. Turner, G.J. Cooney, M. Kolanczyk, K.N. North, D.G. Little, A. Schindeler, NF1 is a critical regulator of muscle development and metabolism, Hum. Mol. Genet. 23 (2014) 1250–1259.
[21] W.C. Liang, I. Nishino, Lipid storage myopathy, Curr. Neurol. Neurosci. Rep. 11 (2011) 97–103.
[22] R.L. Perry, M.H. Parker, M.A. Rudnicki, Activated MEK1 binds the nuclear MyoD transcriptional complex to repress transactivation, Mol. Cell 8 (2001) 291–301.
[23] F. Penna, D. Costamagna, A. Fanzani, G. Bonelli, F.M. Baccino, P. Costelli, Muscle wasting and impaired myogenesis in tumor bearing mice are prevented by ERK inhibition, PLoS One 5 (2010) 0013604.
[24] C.M. Prado, T. Bekaii-Saab, L.A. Doyle, S. Shrestha, S. Ghosh, V.E. Baracos, M.B. Sawyer, Skeletal muscle anabolism is a side effect of therapy with the MEK inhibitor: selumetinib in patients with cholangiocarcinoma, Br. J. Cancer 106 (2012) 1583–1586.
[25] A.P. Brown, T.C. Carlson, C.M. Loi, M.J. Graziano, Pharmacodynamic and toxicokinetic evaluation of the novel MEK inhibitor, PD0325901, in the rat following oral and intravenous administration, Cancer Chemother. Pharmacol. 59 (2007) 671–679.
[26] J. El-Hoss, M. Kolind, M.T. Jackson, N. Deo, K. Mikulec, M.M. McDonald, C.B. Little, D.G. Little, A. Schindeler, Modulation of endochondral ossification by MEK inhibitors PD0325901 and AZD6244 (Selumetinib), Bone 59 (2014) 151–161.
[27] W.J. Jessen, S.J. Miller, E. Jousma, J. Wu, T.A. Rizvi, M.E. Brundage, D. Eaves, B. Widemann, M.O. Kim, E. Dombi, J. Sabo, A. Hardiman Dudley, M. Niwa-Kawakita, G.P. Page, M. Giovannini, B.J. Aronow, T.P. Cripe, N. Ratner, MEK inhibition exhibits efficacy in human and mouse neurofibromatosis tumors, J. Clin. Invest. 123 (2013) 340–347.
[28] N. Kossler, S. Stricker, C. Rodelsperger, P.N. Robinson, J. Kim, C. Dietrich, M. Osswald, J. Kuhnisch, D.A. Stevenson, T. Braun, S. Mundlos, M. Kolanczyk, Neurofibromin (Nf1) is required for skeletal muscle development, Hum. Mol. Genet. 20 (2011) 2697–2709.
[29] F.C. Yang, D.A. Ingram, S. Chen, Y. Zhu, J. Yuan, X. Li, X. Yang, S. Knowles, W. Horn, Y. Li, S. Zhang, Y. Yang, S.T. Vakili, M. Yu, D. Burns, K. Robertson, G. Hutchins, L.F. Parada, D.W. Clapp, Nf1-dependent tumors require a microenvironment containing Nf1 +/− − and c-kit-dependent bone marrow, Cell 135 (2008) 437–448.
[30] M.E. Scholz, J.D. Meissner, R.J. Scheibe, P.K. Umeda, K.C. Chang, G. Gros, H.P. Kubis, Different roles of H-ras for regulation of myosin heavy chain promoters in satellite cell-derived muscle cell culture during proliferation and differentiation, Am. J. Phys. Cell Phys. 297 (2009) 22.
[31] M. Logan, J.F. Martin, A. Nagy, C. Lobe, E.N. Olson, C.J. Tabin, Expression of Cre Recombinase in the Developing Mouse Limb Bud Driven by a Prxl Enhancer Genesis (New York, N.Y.: 2000), vol. 33, (2002), pp. 77–80.
[32] L. Kassar-Duchossoy, E. Giacone, B. Gayraud-Morel, A. Jory, D. Gomes, S. Tajbakhsh, Pax3/Pax7 mark a novel population of primitive myogenic cells during development, Genes Dev. 19 (2005) 1426–1431.
[33] J. El-Hoss, T. Cheng, E.C. Carpenter, K. Sullivan, N. Deo, K. Mikulec, D.G. Little, A. Schindeler, A combination of rhBMP-2 (recombinant human bone morphogenetic protein-2) and MEK (MAP kinase/ERK kinase) inhibitor PD0325901 increases bone formation in a murine model of neurofibromatosis type I pseudarthrosis, J. Bone Joint Surg. Am. 96 (2014) e117.
[34] A. Schindeler, M.M. McDonald, P. Bokko, D.G. Little, Bone remodeling during fracture repair: the cellular picture, Semin. Cell Dev. Biol. 19 (2008) 459–466.
[35] J. El-Hoss, K. Sullivan, T. Cheng, N.Y. Yu, J.D. Bobyn, L. Peacock, K. Mikulec, P. Baldock, I.E. Alexander, A. Schindeler, D.G. Little, A murine model of neurofibromatosis type 1 tibial pseudarthrosis featuring proliferative fibrous tissue and osteoclast-like cells, J. Bone Miner. Res. 27 (2012) 68–78.
[36] J. von Maltzahn, A.E. Jones, R.J. Parks, M.A. Rudnicki, Pax7 is critical for the normal function of satellite cells in adult skeletal muscle, Proc. Natl. Acad. Sci. U. S. A. 110 (2013) 16474–16479.
[37] M.A. Summers, T. Rupasinghe, E.R. Vasiljevski, F.J. Evesson, K. Mikulec,

L. Peacock, K. Gr Quinlan, S.T. Cooper, U. Roessner, D.A. Stevenson, D.G. Little, A. Schindeler, Dietary intervention rescues myopathy associated with neurofibromatosis type 1, Hum. Mol. Genet. 27 (4) (Feb 15 2018) 577–588, http://dx.doi.org/10.1093/hmg/ddx423.

[38] D.H. Gutmann, R.T. Geist, D.E. Wright, W.D. Snider, Expression of the neurofibromatosis 1 (NF1) isoforms in developing and adult rat tissues Cell, Growth Differ. 6 (1995) 315–323.

[39] Y. Zhu, M.I. Romero, P. Ghosh, Z. Ye, P. Charnay, E.J. Rushing, J.D. Marth, L.F. Parada, Ablation of NF1 function in neurons induces abnormal development of cerebral cortex and reactive gliosis in the brain, Genes Dev. 15 (2001) 859–876.

[40] J. Schindelin, I. Arganda-Carreras, E. Frise, V. Kaynig, M. Longair, T. Pietzsch, S. Preibisch, C. Rueden, S. Saalfeld, B. Schmid, J.Y. Tinevez, D.J. White, V. Hartenstein, K. Eliceiri, P. Tomancak, A. Cardona, Fiji: an open-source platform for biological-image analysis, Nat. Methods 9 (2012) 676–682.